Available online at www.sciencedirect.com
SCIENCE DIRECT®
Geotextiles and Geomembranes 23 (2005) 234–260
Geotextiles and Geomembranes
www.elsevier.com/locate/geotexmem

Design and behaviour of a geosynthetic reinforced retaining wall and bridge abutment on a yielding foundation

Graeme D. Skinner[a,*], R. Kerry Rowe[b]

[a]*Golder Associates Ltd., 1000, 940-6th Avenue S.W., Calgary, Alta., Canada T2P 3T1*
[b]*Department of Civil Engineering, GeoEngineering Centre at Queen's-RMC, Ellis Hall, Queen's University, Kingston, Ont., Canada K7L 3N6*

Received 18 January 2004; received in revised form 1 October 2004; accepted 5 October 2004
Available online 26 November 2004

Abstract

There has recently been an increase in the use of geosynthetic reinforced soil structures to support bridge abutments and approach roads in place of traditional pile supports. In this respect, reinforced soil walls offer a cost effective alternative to, and have been found to reduce the "bridge bump" effect associated with, pile supported abutments. The paper focuses on the numerical analysis of a hypothetical 6 m high geosynthetic reinforced soil wall supporting a bridge abutment and approach road constructed on a 10 m thick yielding clayey soil deposit. The results of the numerical analysis are compared to current design methodologies to examine the effect of the yielding soil foundation on the behaviour of the wall and abutment. The study includes the examination of both the internal and external stability of the wall, and focuses on methods of improving the external stability.

Keywords: Geosynthetic reinforcement; Soil wall; Bridge abutment; Soft foundation; Numerical analysis

*Corresponding author. Tel.: +1 403 299 5600; fax: +1 403 299 5606.
E-mail address: graeme_skinner@golder.com (G.D. Skinner).

0266-1144/$ - see front matter © 2004 Elsevier Ltd. All rights reserved.
doi:10.1016/j.geotexmem.2004.10.001

1. Introduction

There has recently been an increase of interest in the construction of reinforced soil retaining walls to supporting bridge abutments in place of traditional pile foundations. Two of the main reasons for the increased interest are the reduction in overall cost of the project and the reduction, or potential elimination, of "bridge bumps" which arises from differential settlement between a traditional pile supported abutment and the approach road (Abu-Hejleh et al., 2002; Helwany et al., 2003).

The majority of recent investigations of the use of geosynthetic (Adams, 2000; Bloomfield et al., 2001; Esta, 2001; Uchimura et al., 2001; Abu-Hejleh et al., 2002; Helwany et al., 2003) and steel (Troung et al., 2001) reinforced soil structures for road and bridge abutment applications were founded on competent materials and performed well under the applied loading conditions. However, there has been very limited research into the behaviour of reinforced soil bridge abutments constructed on time-dependent yielding foundation deposits.

A number of walls (Bloomfield et al., 2001) have been constructed on low shear strength/compressible soil deposits where additional measures were taken to improve the external stability and decrease the potential for large settlement. These measures included the use of staged construction, pre-loading and surcharge loading, in conjunction with the use of vertical drains. Given adequate time, this allowed consolidation to occur before and during wall construction, thus increasing the undrained shear strength and short-term external stability, and allowed consolidation settlements to occur before the end of construction in order to decrease the overall end of construction settlements. In addition to these considerations, a high strength geogrid layer was used at the base of one wall to increase the external stability. It was found that all of the walls performed well despite the adverse foundation conditions. Finally, it has been shown by numerical investigation (Helwany et al., 2003) that the performance of a reinforced soil bridge abutment can be significantly affected by the behaviour of the foundation soil deposit.

Therefore, it was of interest to investigate the behaviour of a geosynthetic reinforced soil wall and bridge abutment constructed on a viscoplastic foundation soil and, in particular, to examine the effects of yielding on the behaviour of the structure. To this end, a bridge abutment and approach road were assumed to act at the top of a typical reinforced soil wall with two different loading scenarios: the first considered the abutment and road dead loads alone; and the second included a sustained traffic load in addition to the dead loads (Fig. 1). In order to examine the effect of significant yielding in the foundation soil during and after the additional loads were applied, but not external failure, the two loading cases were selected such that they decreased the external factors of safety below the minimum values required by the National Concrete Masonry Association (National Concrete Masonry Association (NCMA), 1996), but had a factor of safety greater than unity.

The primary objective of this study is to examine the short- and long-term effects of increasing the foundation yielding, due to the additional loading associated with a bridge abutment and sustained traffic, on the behaviour of a reinforced soil wall. A

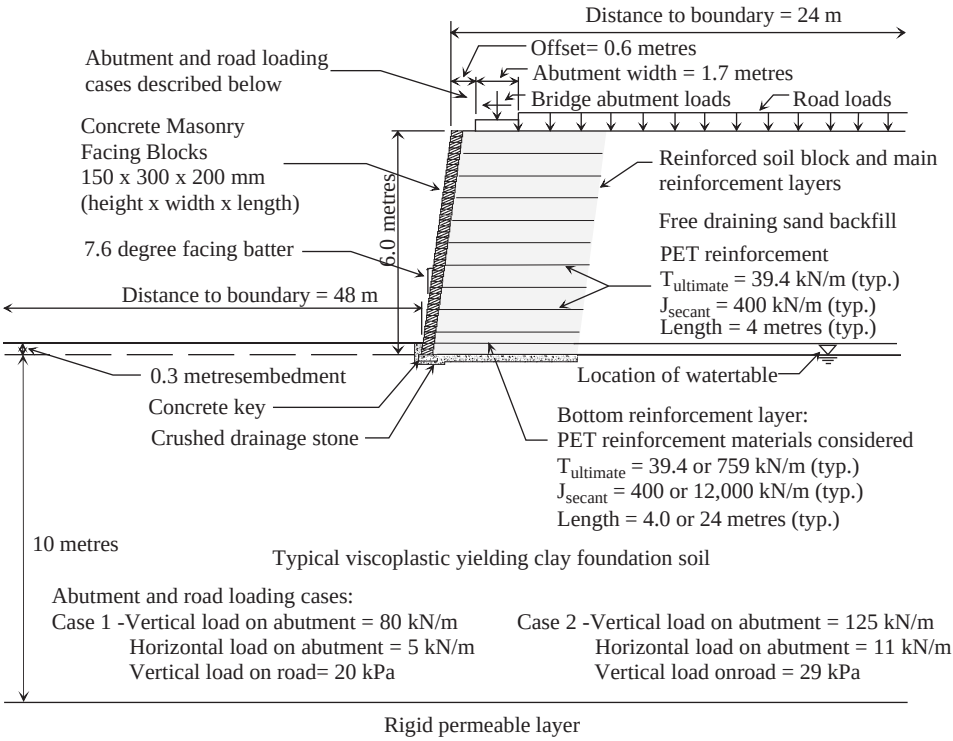

Fig. 1. Cross-section of typical wall with bridge abutment and approach road loads.

secondary objective is to examine the implications of this behaviour with respect to current design methodologies (National Concrete Masonry Association (NCMA), 1996) in terms of both stability and deformations, and to investigate the effect of increasing the length and stiffness of the bottom reinforcement layer on the external stability of the wall.

2. Numerical model

A version of the finite-element (FE) program AFENA originally developed by Carter and Balaam (1990) and modified as noted below to account for both the modelling of geosynthetic reinforced soil walls and viscoplastic clay behaviour was used to conduct the numerical analyses reported herein. The soil retaining wall was examined under two-dimensional (plane strain) conditions consistent with normal design assumptions (Canadian Foundation Engineering Manual (CFEM), 1992; Federal Highway Administration (FHWA), 1996; National Concrete Masonry Association (NCMA), 1996). The finite-element mesh used 4335 eight noded isoparametric elements to model the soil, masonry and concrete, 288 linear bar

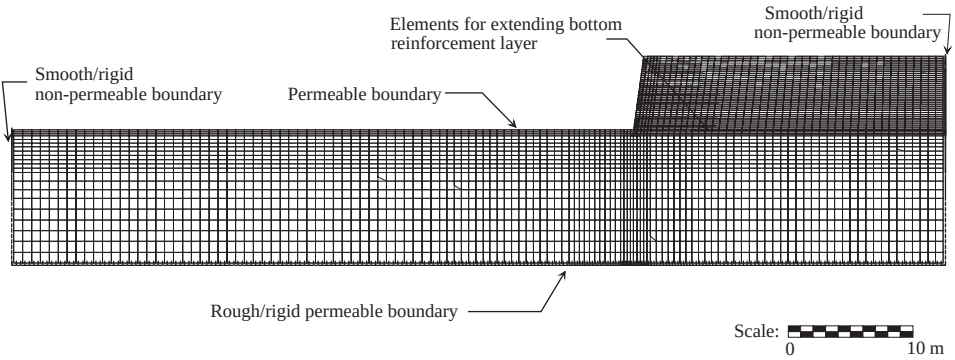

Fig. 2. FE mesh.

elements (with no significant compressive or bending strength) to model the reinforcement and 1390 interface elements were used between the various materials (Fig. 2). The initial geostatic stress conditions in the foundation were based on the unit weight and effective coefficient of lateral earth pressure at rest (K_0) for the soil.

The viscoplastic model adopted for the continuum elements used for the clay foundation combined an elliptical cap yield surface (Chen and Mizuno, 1990) and a Drucker–Prager failure criterion with Perzyna's (1963) over-stress model and fully coupled Biot (1941) type consolidation (Rowe and Hinchberger, 1998).

An elasto-plastic stress–strain model with a Mohr–Coulomb failure criterion was adopted for the continuum elements used for the coarse-grained soils, masonry facing and concrete key. Young's modulus, E, of the granular soils was assumed to be non-linear and given by Janbu's (1963) equation expressed in the form

$$\frac{E}{P_a} = K\left(\frac{\sigma_3}{P_a}\right)^n, \tag{1}$$

where σ_3 is the minor principle stress, P_a is the atmospheric pressure (e.g. 101.3 kPa), the values of K and n were selected based on correlations (Duncan et al., 1980) with the assumed soil properties. To deal with the case of low σ_3, a minimum stiffness was assumed equal to $K(P_a)^n$, since at no times would the stiffness of the confined coarse-grained materials be close to zero in this study. The masonry and concrete materials were assumed to be purely elastic materials.

Rigid–plastic interface elements, as described by Rowe and Soderman (1987), were used to model the behaviour between the various materials. A Mohr–Coulomb failure criterion was used to model failure at interfaces.

The model adopted had been previously used to successfully describe the behaviour of a full-scale reinforced soil wall (Rowe and Skinner, 2001), the geosynthetic reinforced Sackville test embankment (Rowe and Hinchberger, 1998), and in the numerical analysis of reinforced embankments constructed on viscoplastic foundation soils (Li and Rowe, 1999; Li, 2000).

The wall construction was simulated layer-by-layer and it was assumed that the wall and abutment construction occurred over 24 and 122 day periods, respectively.

The additional sustained traffic load was applied as a linearly increasing load over an assumed 6 h period at which point it remained constant with time. Although traffic loads are normally considered as transient live loads, in this case it represented an additional sustained load equivalent to constant traffic on the bridge. The non-linear and time-dependent analysis of the wall and abutment construction, abutment loading and subsequent consolidation behaviour was performed in sufficiently small increments to ensure numerical stability of the solution and to minimize numerical errors (Skinner, 2002).

A limit-equilibrium analysis was conducted to ensure adequate distance between the bottom rough/rigid and right lateral smooth/rigid boundaries and the primary zone of influence of the wall, modelled at distances of 10 m from the base of the wall and 24 m from the top edge of the wall face, respectively. The distance to the left lateral smooth/rigid boundary was assumed to be at least ten times the initial length of the reinforcement to minimize boundary effects as discussed by Rowe and Skinner (2001). Finally, the top and bottom of the clay layer were assumed to be zero excess pore pressure seepage boundaries.

3. Model parameters and design considerations

3.1. Design and description of wall with abutment loads

The wall was designed based on the current NCMA working stress design code (National Concrete Masonry Association (NCMA), 1996) for segmental walls. This approach specifically considers a segmental wall facing and is based on Coulomb's active earth pressure theory. The wall was designed to a height of 6 m with ten layers of 4 m long knitted polyester (PET) geogrid. The facing was assumed to be constructed from 40 masonry-facing blocks (e.g. Pisa II blocks from Unilock®) each having an infilled unit weight of 21.8 kN/m^3 and a natural setback of 20 mm due to interlocking shear keys. The wall was embedded 0.3 m (Fig. 1). A prefabricated concrete key and gravel layer were used at the toe and base of the wall, respectively. The concrete key acted as a levelling surface for face alignment only and served no structural purpose. The thin (0.15 m) layer of gravel at the base of the reinforced wall and around the key acted as a level surface for construction of the wall and the top drainage boundary for the clay foundation below the wall. The watertable was assumed to be located at the top of the clay foundation. The block/block and block/reinforcement interface parameters are given in Table 1.

The allowable reinforcement tensile strength was assumed to be 20.4 kN/m (Geotechnical Fabrics Report (GFR), 1999 for Stratagrid 200) and accounted for the ultimate and creep limited tensile strength of the geogrid, and additional strength reductions due to installation damage and durability as indicated in Table 1. The geogrid secant tensile stiffness, J, was taken to be 400 kN/m based on ASTM Standard D 4595 (1998) and Bathurst (2000). The polyester geogrid was assumed to have limited susceptibility to creep deformation (Koerner, 1990).

Table 1
Geosynthetic material properties

Material property	Test methodology	Value
Ultimate tensile strength (kN/m)	ASTM Standard D 4595, 1998	39.7
Creep tensile strength (kN/m)	ASTM Standard D 5262, 1998	24.6[a]
Allowable tensile strength (kN/m)	GRI GG4, 1991	20.4[b]
Tensile stiffness, 'J' (kN/m)	ASTM Standard D 4595, 1998	400

[a]Creep reduction factor = 1.61.
[b]Installation reduction factor = 1.05, durability reduction factor = 1.15 and overall reduction factor = 1.0.

Table 2
Sand and drainage gravel material parameters

Characteristic	Sand backfill	Drainage gravel
Unit weight (kN/m^3)	20	20
Friction angle (deg)	35	45
Dilation angle (deg)	6	12.5
Poisson's ratio, v	0.3	0.35
Coefficient of earth pressure at rest, K_0	0.4	0.3
Janbu K and n	460, 0.5	900, 0.7

The reinforced and retained backfill were assumed to be the same cohesionless sand and the drainage layer at the base of the wall was assumed to be cohesionless gravel. The unit weight, friction and dilation angles, and other assumed parameters for the sand and gravel are given in Table 2. All parameters were taken from the range of typical values for these materials (Craig, 1992; Holtz and Kovacs, 1981), with the following exceptions. The dilation angle of each material was assumed to be given by Bolton's (1986) equation $\psi' = (\phi' - \phi'_{cv})/0.8$, where the value of the constant volume friction angle (ϕ'_{cv}) was assumed to be 30° and 35° for the sand and gravel, respectively (Craig, 1992). The non-linear Janbu (1963) stiffness parameters K and n were selected for the assumed soil properties based on Duncan et al. (1980).

The block/block interface parameters were estimated from test protocol SRWU-1 (National Concrete Masonry Association (NCMA), 1996) for both the ultimate and serviceability criterions, as reported by Bathurst et al. (1996), and are given in Table 3. The interface friction angle between the facing blocks and the backfill soil was taken as two-thirds the sand friction angle. The same assumption was made for the interface between the gravel soil and both the facing blocks and concrete key based on the gravel material. The interface between the backfill and the foundation was assumed to be equal to the normally consolidated friction angle of the foundation, since it was the lesser value for the two soils. The interface friction between the backfill soil and reinforcement was taken as 90% of the backfill friction based on similar material parameters (Krieger and Thamm, 1991), rather than the

Table 3
Material interface parameters

Interface	Criterion	Minimum shear force (kN/m)	Friction angle (deg)
Block/block	Ultimate strength	11.5	59
	Serviceability state	9.4	51
Backfill/facing block	Ultimate strength	0	23.3
Backfill/reinforcement	Ultimate strength	0	31.5
Backfill/foundation	Ultimate strength	0	27
Gravel/concrete key	Ultimate strength	0	30
Embedment/facing block	Ultimate strength	0	30

conservative assumption of 70% indicated by NCMA (1996) for the case where no other data is available. The interface friction angles between the various materials are summarized in Table 3.

The minimum reinforcement length and wall embedment depth were taken as 0.6 times the height of the wall and the exposed height of the wall divided by 20, respectively, as specified by the NCMA (1996) manual. Further, the maximum reinforcement spacing was limited to two times the facing block width, as recommended by the American Association of State Highways and Transportation Officials (AASHTO) (1996). The design coefficient for sliding for the geogrid reinforcement was taken as 0.95 (National Concrete Masonry Association (NCMA), 1996).

The assumed bridge abutment and road loads were based on an example in the Federal Highways Administration (FHWA) design manual (Federal Highway Administration (FHWA), 1996) with an assumed abutment width of 1.7 m and offset of 0.6 m from the front of the wall (Fig. 1). Two loading cases were considered to act along the top of the wall. The first (Case 1) represented a lightly used road with an approximate transient traffic load, thus only the abutment and road dead loads were accounted for at the top of the wall. The second (Case 2) represented a heavily travelled road with an approximately constant volume of traffic, thus a sustained traffic load was included in addition to the abutment and road dead loads. The assumed loads are given in Table 4.

The NCMA manual (1996) does not explicitly consider the stability of the abutment on top of the retaining wall or the associated abutment and road forces as part of the internal and external stability calculations. Thus, the stability of abutment was estimated following the FHWA manual (1996) and was found to be satisfactory. For the stability design of the wall, the abutment and road were assumed to act as a strip footing (Federal Highway Administration (FHWA), 1996; Bathurst and Jones, 2001) and an offset uniformly distributed load (Craig, 1992), respectively.

The NCMA manual (1996) covers a wide range of potential internal and facing failure modes, and considers the interface characteristics between the various

Table 4
Abutment loads (modified from Federal Highway Administration (FHWA), 1996)

Case 1 (dead loads only)	Magnitude
Vertical load from abutment (kN/m)	80
Horizontal load from abutment (kN/m)	5
Vertical load from road (kPa)	20
Case 2 (Case 1 + traffic live load)	**Magnitude**
Vertical load from abutment (kN/m)	125
Horizontal load from abutment (kN/m)	11
Vertical load from road (kPa)	29

materials. The internal stability of the wall accounting for Cases 1 and 2 loadings was governed by the pullout resistance of the reinforcement, the connection strength between the reinforcement and facing blocks, and the maximum reinforcement spacing. The reinforcement was placed at the maximum spacing of twice the facing block length (0.6 m), and was taken to be 4.0 m in length (greater than the minimum required length of 3.6 m) to increase the overall pullout resistance, and an additional layer of reinforcement was added at a height of 0.3 m to prevent pullout failure of the layer above it. 'Positive' or mechanical connections (e.g. pins, dowels or clips from National Concrete Masonry Association (NCMA), 1996) were assumed between the reinforcement and facing blocks to satisfy the facing connection stability criterion. These 'positive' connections represented a 100% connection capacity between the reinforcement and facing blocks and were thus limited by the allowable strength of the reinforcement (Skinner, 2002). The external stability was based on the assumed foundation conditions discussed below.

3.2. Foundation description and design stability

The 10 m thick foundation deposit was taken to be a viscoplastic yielding clay similar to that described by Li and Rowe (1999) with properties as given in Table 5. The initial void ratios were taken to be 2.0–1.75 (from top to bottom of the deposit), and the average unit weight was 15.8 kN/m^3. The vertical hydraulic conductivity was assumed to be a function of the void ratio given by the equation

$$k_v = k_{vo} \times \exp\left(\frac{e - e_0}{C_k}\right), \tag{2}$$

where the initial vertical hydraulic conductivity (k_{v0}) and void ratio (e_0) are given in Table 5 and the hydraulic conductivity change index (C_k) was taken to be 0.5 for both cases (based on Mesri et al., 1994). Recognizing that typically the hydraulic conductivity of clay is anisotropic (Tavenas et al., 1983; Terzaghi et al., 1996), the ratio of horizontal to vertical hydraulic conductivity was assumed to be $k_h/k_v = 3$. The viscoplastic characteristics were based on the rate-dependent relationship

Table 5
General foundation material properties

Property	Value
Specific gravity	2.74
Liquid limit (%)	76
Plasticity index	40
Initial void ratio (top to bottom of deposit)	2.0–1.75
Average unit weight (kN/m^3)	15.8
Compression index (C_c)	0.69
Recompression index (C_r)	0.069
N/C friction angle (deg)	27
N/C cohesion (kPa)	0
O/C friction angle (deg)	20
Coefficient of earth pressure at rest (K_0)	0.6
Poisson's ratio (v)	0.35
Elliptical cap aspect ratio (R_c)	1.2
Initial hydraulic conductivity (k_{v0} (m/s)	1×10^{-9}
Hydraulic conductivity constant (C_k)	0.5
Ratio of horizontal to vertical hydraulic conductivity (k_h/k_v)	3
Viscoplastic fluidity constant (/h)	1.0×10^{-7}
Viscoplastic strain rate exponent	30
Preconsolidation pressure at top of layer (kPa)	93
Change in preconsolidation pressure with depth (kPa/m)	4.5
Undrained shear strength at top of layer[a] (kPa)	50.3
Change in undrained shear strength with depth[a] (kPa/m)	0.9

[a]Based on the estimated corrected (Bjerrum, 1973) shear vane results.

between undrained shear strength and strain rate presented by Kulhawy and Mayne (1990) and estimated by Li (2000). All other relevant soil properties are summarized in Table 5. The initial vertical effective stress and preconsolidation pressure profiles are shown in Fig. 3. Based on the assumed parameters and accounting for the relationship between plane strain and corrected (Bjerrum, 1973) field vane strengths (Skinner, 2002), the corrected undrained shear vane strength at the top of the foundation stratum, s_{uo}, was calculated from the viscoplastic cap model (Rowe and Hinchberger, 1998) to be 50.3 kPa and increased with depth at a rate of 0.9 kPa/m, as shown in Fig. 3.

For this study, the external stability was governed by the short-term bearing capacity and global stability analyses. The method of bearing capacity analysis specified by the NCMA manual (1996) considers the reinforced soil wall to act as a rigid block with a reduced bearing area due to eccentricity and requires a minimum factor of safety of 2. The short-term ultimate bearing capacity of the foundation may be estimated from the corrected (Bjerrum, 1973) field vane shear strength profile, and the bearing capacity solutions published by Davis and Booker (1973). The manual recommends the method of slices for estimating global stability and therefore a limit equilibrium analysis using Spencer's method (as programmed into Slope/W, 2001), accounting for both force and moment equilibrium, was conducted. As a result of

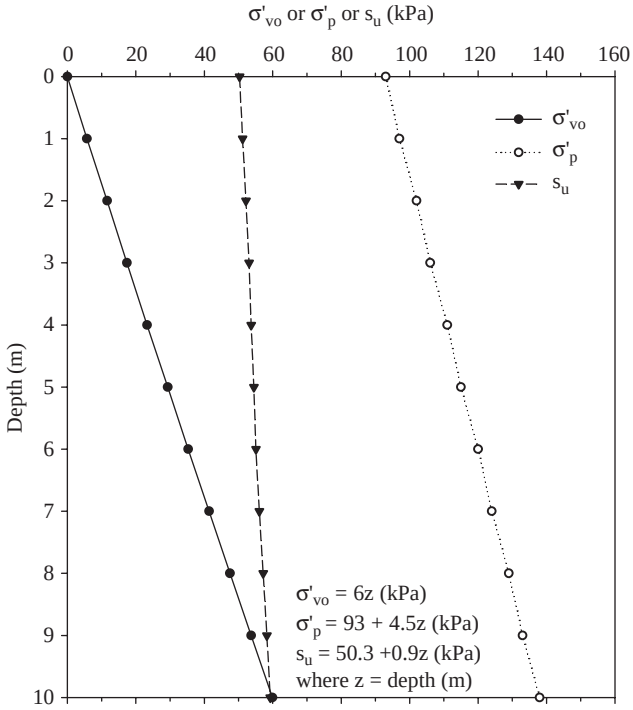

Fig. 3. Initial effective stress, preconsolidation pressure and undrained shear strength of clay foundation soil (s_u = Bjerrum (1973) corrected shear vane strength).

Table 6
External bearing capacity and global stability factors of safety

Case	Description	Bearing capacity FS_{min}[a] = 2.0	Global stability FS_{min}[a] = 1.5
	Wall alone	2.0	1.8
1	Abutment and road dead loads	1.8	1.5
2	Case 1 + sustained traffic load	1.5	1.4

[a]Minimum factor of safety from NCMA (1996).

the additional abutment and road loads the external bearing capacity of Cases 1 and 2 and the global stability of Case 2 were less than the minimum required factors of safety as summarized in Table 6. Although these cases does not represent adequate design scenarios where the minimum factors of safety would be met, they do allow for the investigation of the effects of significant foundation yielding on the behaviour

of a reinforced soil wall. They may be thought to represent situations where the foundation stiffness and strength has been over-estimated, or additional loading is added to the wall after it as been initially designed and constructed. As well, they allow for the investigation of the effect of increasing the length and stiffness of the bottom reinforcement layer on the external stability of the wall.

4. Results of analysis of wall under additional loading cases

The results of the FE analyses for loading Cases 1 and 2 were the same up to the end of adding the abutment and road dead loads. After this point, for Case 1 no other loads are added and the behaviour of the wall was examined until 95% consolidation was reached. For Case 2 the additional sustained traffic load was then added to the abutment and road dead loads and the behaviour of the wall was again examined until 95% consolidation (7 years in both cases) was reached. In addition, the behaviour of the wall alone, with no additional loads, was examined until 95% consolidation (7 years) was reached. It should be noted that the degrees of consolidation (i.e. 95% consolidation) discussed in this study are for a point along the right lateral boundary, half-way between the top and bottom drainage boundaries. This point was used to represent the lowest degree of consolidation at any time within the clay foundation deposit, and the associated average degree of consolidation along the right lateral boundary was slightly greater than the value given at the point of interest for each case.

It was found there was no significant effect from the potential generation of additional excess porewater pressure within the viscoplastic clay foundation yield zone below the backfill soil at any time for all cases examined in this study.

4.1. Foundation behaviour and stability

At the end of wall construction (EOWC), the foundation was stable and displayed a shallow potential slip surface. The stress state of most of the soil below the wall was beyond the initial static yield surface (due to the viscoplastic over-stress model used in this study) and in a state of over consolidated (O/C) yield (Fig. 4). It should be noted that the model is capable of accounting for both normally and O/C yielding of a soil beyond the elastic range and before ultimate failure occurs (Atkinson and Bransby, 1978). During the time Case 1 loading was applied, the stress state of the soil below the wall moved into a state of normally consolidated (N/C) yield or failure (Fig. 5). One can see the first step towards the development of a potential shear failure zone as the N/C failure zone extends through the foundation soil from the toe and around the base of the reinforced soil wall due to the construction and additional loads at the minimum factor of safety of 1.5 (global stability).

When Case 1 loading alone was applied over an assumed 122-day period, the wall remained stable and the velocity vectors and strain rate contours decreased between the EOWC and completion of the application of Case 1 loading. Thus, there was no accelerated movement of the foundation soil with the addition of Case 1 loading.

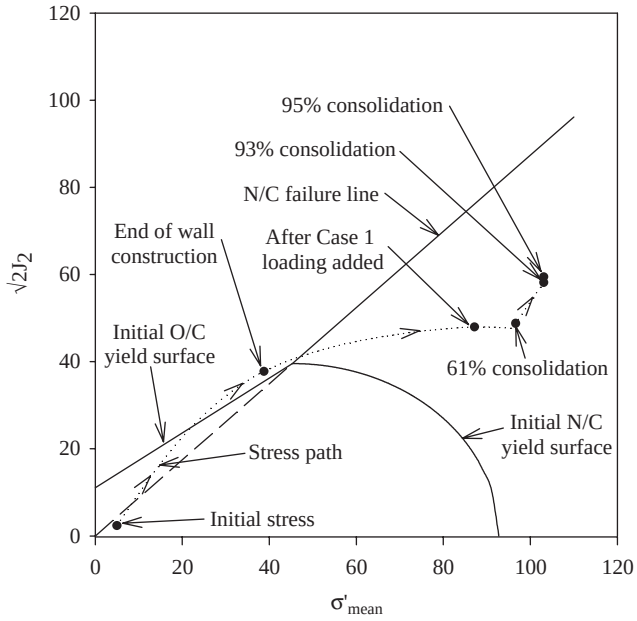

Fig. 4. Stress path at a point 1 m below toe of wall for Case 1 loading.

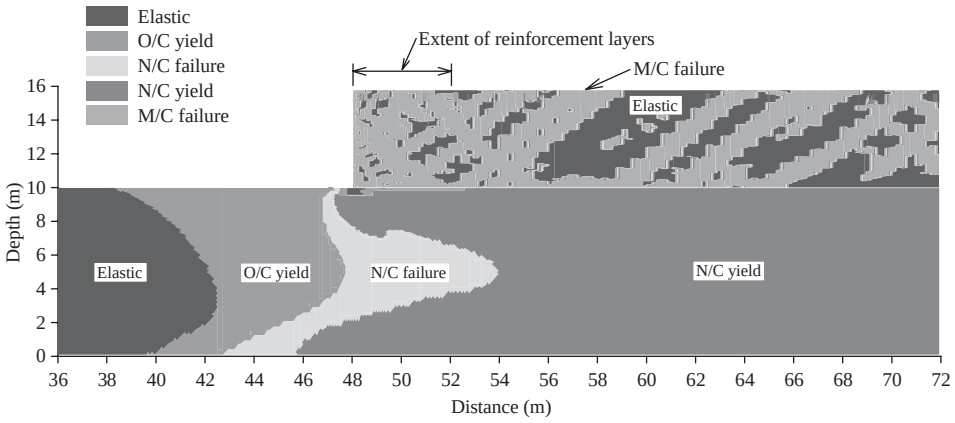

Fig. 5. Plasticity zones in wall and foundation after Case 1 loading applied.

When Case 2 loading was rapidly applied over a 6 h period immediately after Case 1, the N/C failure zone increased in size, and a potential shear failure surface became more evident as it continued to extend below and towards the surface behind the reinforced soil wall (Fig. 6). Although N/C failure zones developed in the foundation for both load cases, the significantly higher application rate and load magnitude of

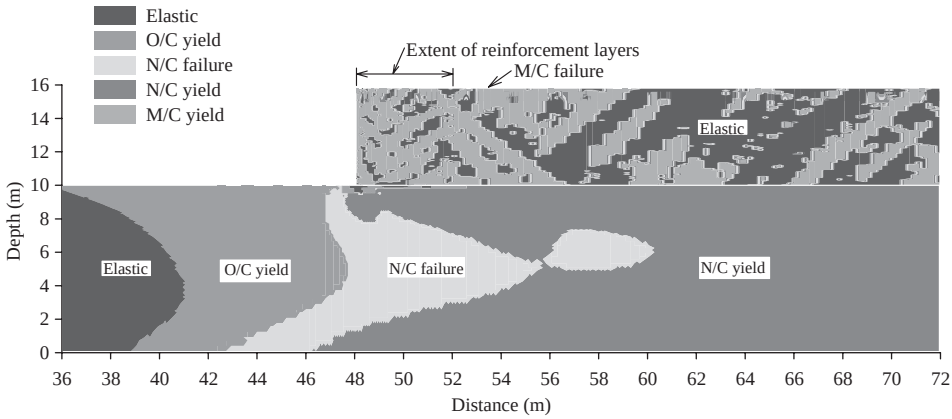

Fig. 6. Plasticity zones after Cases 2 loading was applied.

Case 2 caused a larger N/C failure zone to develop in the foundation. This highlights the importance of construction rate on the stability of a structure on a rate sensitive foundation.

It was found that the wall remained internally and externally stable during the entire analysis to 95% consolidation for both loading cases. Therefore, although the loading cases both had external factors of safety below the minimum required by the NCMA (1996) design code and caused N/C failure zones to develop within the foundation, the factors of safety were 1.4 or greater and the foundation had sufficient strength to maintain the stability of the wall under both abutment and traffic loads.

4.2. Wall and foundation deformations

The displacements at the top, face and base of the wall were significant in magnitude after Cases 1 and 2 loadings were applied and at 95% consolidation (Figs. 7–9, respectively), and the overall displacements were greater for Case 2 due to its higher loads. The total vertical and horizontal displacements were highest at the top and face of the wall at 95% consolidation for both cases. The vertical displacements were larger at the top of the wall compared to the base due to the combination of the vertical and rotational displacement of the base and the lateral displacement of the wall face. The calculated maximum total displacements at the top and face of the wall were 640 and 430 mm and 970 and 698 mm for Cases 1 and 2, respectively, at 95% consolidation. This represented increases in facing deformation of 540% and 884% for Casess 1 and 2 relative to those at the EOWC, and 300% and 488% relative to those of the wall alone at 95% consolidation. These large deformations were attributed to the combined effect of significant consolidation and yielding of the foundation when the additional loading cases were applied and, due to their significant magnitude, would be in excess of most allowable project

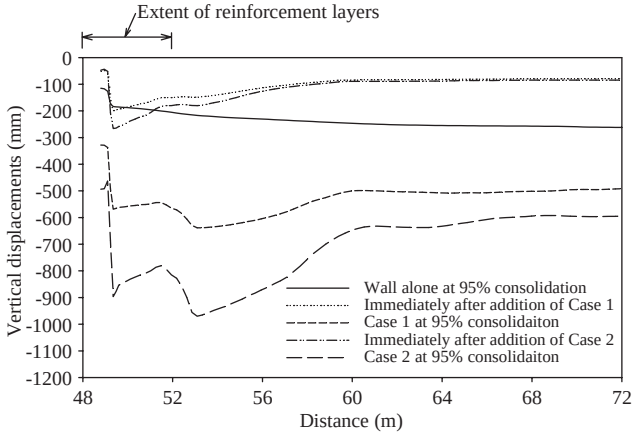

Fig. 7. Vertical displacements at top of wall after Cases 1 and 2 loadings were applied and at 95% consolidation (95% consolidation = % degree of consolidation at a point along right lateral boundary at centre of foundation deposit).

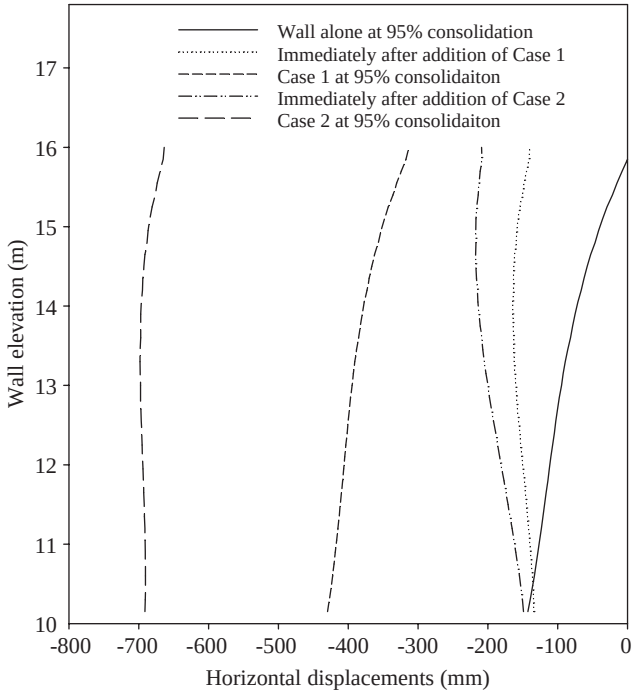

Fig. 8. Horizontal displacements at wall face after Cases 1 and 2 loadings were applied and at 95% consolidation (95% consolidation = % degree of consolidation at a point along right lateral boundary at centre of foundation deposit).

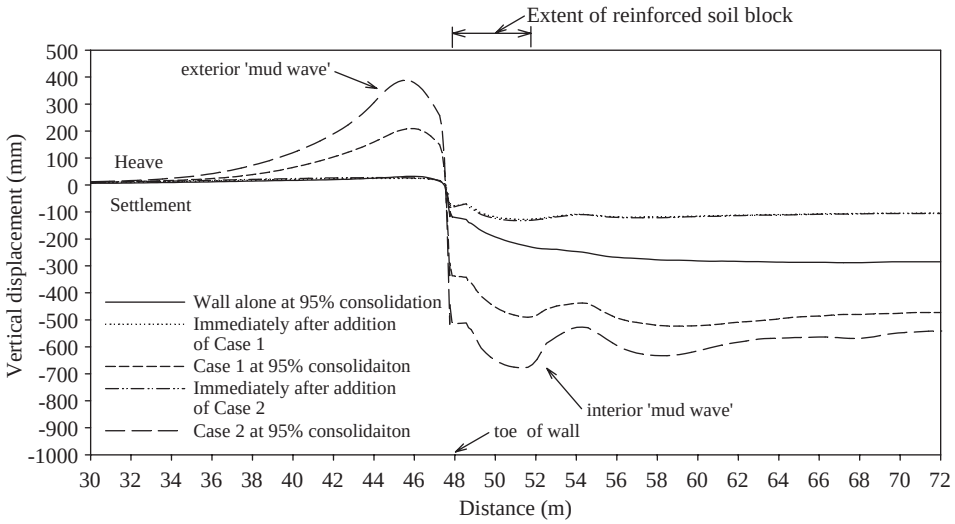

Fig. 9. Vertical displacements at base of wall after Cases 1 and 2 loadings were applied and at 95% consolidation (95% consolidation = % degree of consolidation at a point along right lateral boundary at centre of foundation deposit.

specifications. Although Cases 1 and 2 do not represent typical design situations, this shows that without careful consideration of foundation soil properties and design loading conditions that excessive deformations can occur. From a design point of view it would be difficult to apply a simple method of predicting the top and face deformations since their magnitude is not only a function of the foundation settlement, but also of the stiffness of the facing, backfill and reinforcement materials.

The vertical deformations along the top of the foundation showed the upward displacement of soil in front of and behind the reinforced soil block for Cases 1 and 2 (Fig. 9), and only in front for the wall alone. These 'mud waves' illustrated the outward movement of soil from beneath the reinforced block and the unreinforced backfill section as the foundation soil deposit consolidates and the stiffer backfill soil displaces the clay foundation material.

Even though the wall and foundation together showed large (excessive) displacements, the deformations at the top of the wall were less across the reinforced backfill section than the soil adjacent to it. The differential displacements along the top from the front to the back of the reinforced section were 15 and 40 mm for Cases 1 and 2, respectively, which were significantly less than at the base of the wall where the differential displacements were 154 and 161 mm for Cases 1 and 2, respectively. This behaviour was attributed to the ability of the flexible reinforced soil block to allow larger differential displacements to occur at the base of the wall and not to fully transfer these deformations to the top of the wall as would be the case with a rigid or gravity retaining structure.

4.3. General wall behaviour

The vertical stresses at the base of the reinforced wall were below the expected design (National Concrete Masonry Association (NCMA), 1996) values, except at the toe (Fig. 10). The vertical stress at the toe was 22% higher than the design value for the wall alone, and 27% and 37% higher than the design values for Cases 1 and 2 at 95% consolidation, respectively (an average of 29% higher overall). It should be noted that although the stress for Case 2 had decreased by 95% consolidation due to stress redistribution of the foundation, it was still greater than the design value. The greater stresses at the toe were likely due to the transfer of forces from the backfill soil to the wall face by both friction along the face and through the reinforcement connections as previously discussed by Rowe and Skinner (2001), and this is not accounted for in standard design. It should be noted that the jagged shape of the vertical stress at approximately the 52 m location for all cases was due to the transition in soil materials below the wall backfill from the end of the gravel levelling pad to the clay foundation deposit. The slight increase in the vertical stress at these locations may be attributed to stresses arching to the stiffer gravel material from the clay.

Generally, the horizontal stresses along the back of the wall face were found to be at or below the estimated design active earth pressure (K_a) for the wall alone and

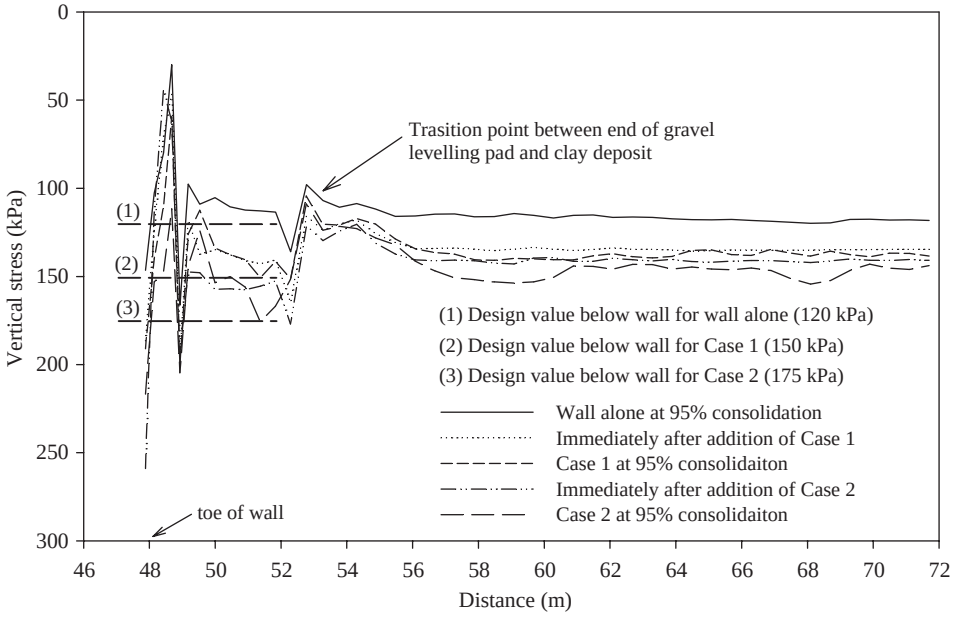

Fig. 10. Vertical stress at base of wall after Cases 1 and 2 loadings were applied and at 95% consolidation (95% consolidation = % degree of consolidation at a point along right lateral boundary at centre of foundation deposit).

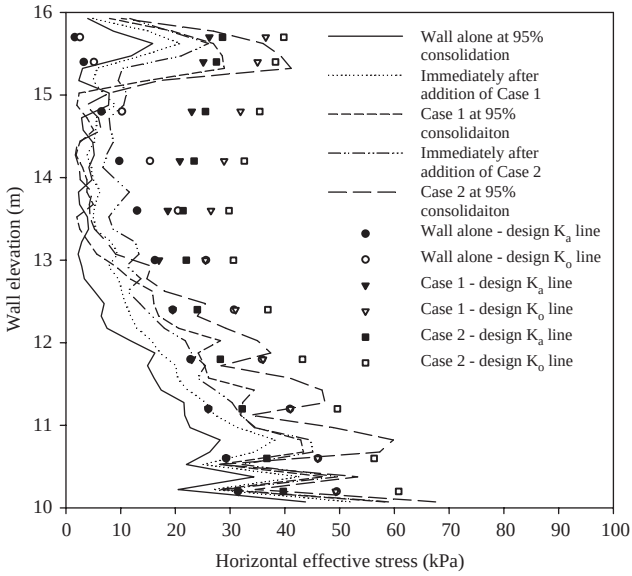

Fig. 11. Horizontal effective stress along back of wall face after Cases 1 and 2 loadings were applied and at 95% consolidation (95% consolidation = % degree of consolidation at a point along right lateral boundary at centre of foundation deposit).

both Cases 1 and 2 (Fig. 11). However, this was not true at two locations. The first was at the bottom of the wall where the horizontal stresses were on average greater than the active pressure and at the very base greater than the at-rest condition for Cases 1 and 2. This increase in horizontal stress was a reflection of the increased vertical stress at the toe of the wall and friction between the base of the wall and the foundation. The second was at the top of the wall where the horizontal stresses exceeded the estimated active pressure from design in all three cases at 95% consolidation due to stress redistribution in the backfill as the foundation deposit consolidated and the additional loadings rotated towards the facing. Although these increases were not considered in the design, the internal factors of safety (that were satisfied in the wall design) would seem to adequately account for them, due to the conservative nature of the design code (Allen and Bathurst, 2002). It should be noted that the jagged shape (increase and decrease) of the horizontal stress along the elevation of the wall face corresponds to the connection locations of the reinforcement layers. The horizontal stresses decrease at the point that the reinforcement connects to the wall face due to arching between the backfill and reinforcement to the stiffer facing blocks.

The strains in reinforcement layers increased with both the addition of Cases 1 and 2 loadings and time (Figs. 12 and 13, respectively). The point of maximum strain in each layer was within the reinforced soil mass and not at the connections. The increase in reinforcement strain was greater at the top portion of the wall with the addition of the abutment and road loads as expected and was partially accounted for

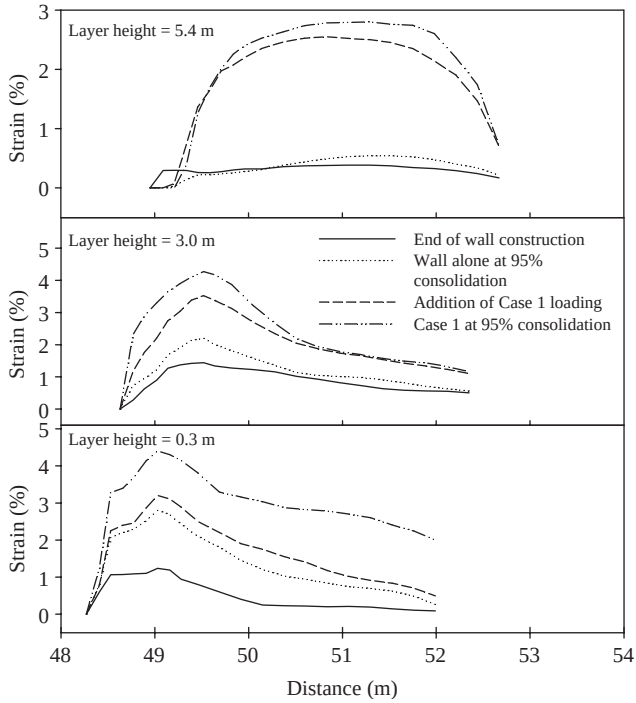

Fig. 12. Strains in various reinforcement layers for Case 1 loading (95% consolidation = % degree of consolidation at a point along right lateral boundary at centre of foundation deposit).

in design. The design method only considered the increase in strain due to the applied load alone and not the associated consolidation and plastic shear deformations of the foundation that further increased the reinforcement layer strain.

At the heights of 0.3, 3.0 and 5.4 m, the maximum strains increased 158%, 150% and 550%, respectively, for Case 1 loading and 175%, 210% and 850% for Case 2 loading from the EOWC to just after the load cases were applied. These increases in strain could be attributed to the additional load cases and the undrained shear deformations of the yielding foundation. The large percent increase in strain in the top reinforcement layer was due to the initially low strain at the EOWC.

After the addition of the loads, the strains continued to increase with time due to foundation settlement, with the greatest increases occurring in the lower layers. The increase in maximum reinforcement strain from the end of the additional loading to 95% consolidation at the same heights were 42%, 23% and 8%, respectively, for Case 1 and 76%, 31% and 18% for Case 2. Overall at the same heights, the increase in maximum reinforcement strain at 95% consolidation compared to the wall alone were 57%, 91% and 418% for Case 1 and 107%, 155% and 733% for Case 2. These increases in strain were due to the increased combination of both primary and secondary consolidation and the plastic shear deformation of the foundation and are

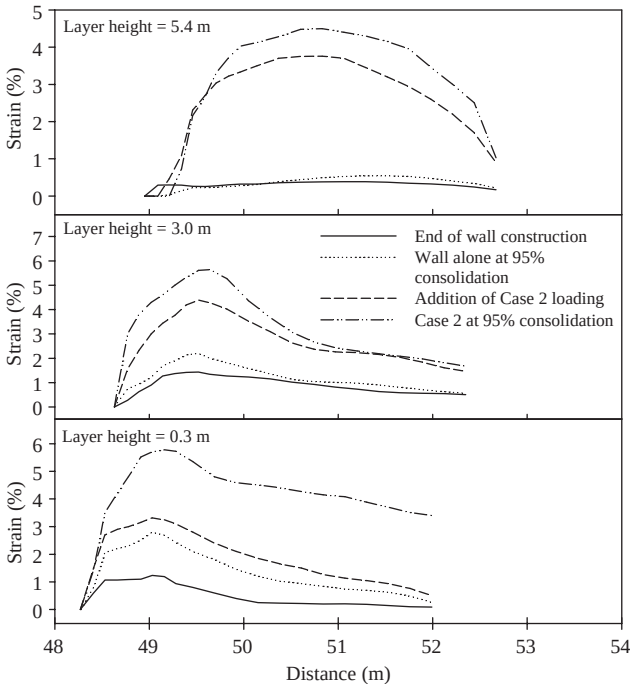

Fig. 13. Strains in various reinforcement layers for Case 2 loading (95% consolidation = % degree of consolidation at a point along right lateral boundary at centre of foundation deposit).

not accounted for in design. This can be illustrated by comparing the FE predicted (at 95% consolidation) and design calculated strain values in the lower half of the wall, with the FE values being between 60% and 90% higher for Case 1 and between 93% and 100% higher for Case 2 than the design calculated strains. Further, the maximum forces in all the reinforcement layers below the height of 3.6 m exceeded the maximum allowable limit at 95% consolidation for Case 2 loading (Fig. 14). Thus, although it has been shown that current design methodology can be conservative for normal working conditions (Allen and Bathurst, 2002), the effects of unanticipated foundation yielding due to under-estimating soil strength and stiffness or the addition of unanticipated load can cause the reinforcement layer forces to exceed their allowable limit.

5. Parametric study of bottom reinforcement layer

The factors of safety from the NCMA (1996) design manual for the bearing capacity of Cases 1 and 2 loadings and the global factor of safety of Case 2 were below the minimum values of 2.0 and 1.5, respectively, as discussed above. In order to increase these factors of safety and overall external stability of the wall, a

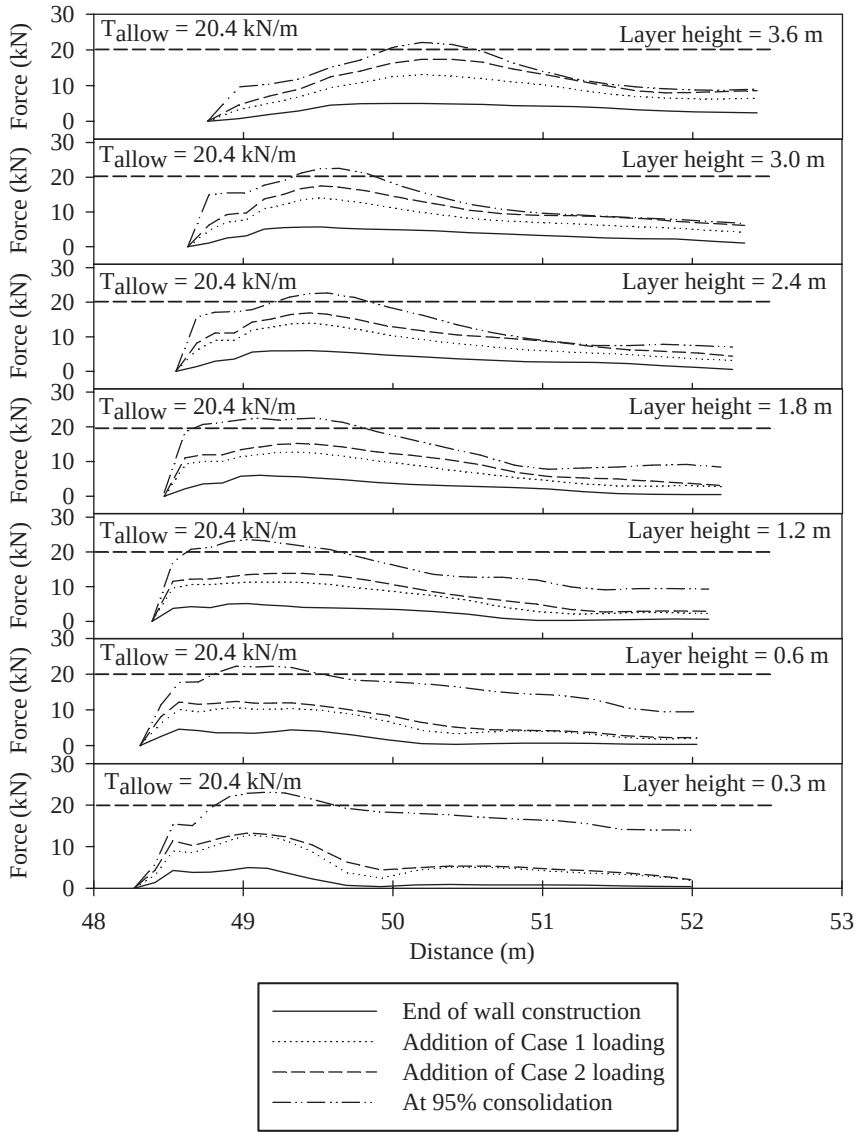

Fig. 14. Forces in reinforcement layers below 3.6 m height for Case 2 loading (95% consolidation = % degree of consolidation at a point along right lateral boundary at centre of foundation deposit).

parametric study of the bottom reinforcement layer (at a height of 0.3 m) was conducted. The study focused on increasing the external stability of the wall by lengthening and stiffening the bottom reinforcement layer and studying the effect on the behaviour of the wall. A number of cases have documented the use of high strength geogrid reinforcement at the base of a reinforced soil wall in order to increase stability and aid in controlling differential settlements (Curtis et al., 1988;

Bloomfield et al., 2001; Troung et al., 2001). Due to the excessive deformations of Case 2, only Case 1 loading was considered herein.

5.1. Lengthening of bottom reinforcement layer

To examine the effect of increasing the length of the bottom reinforcement, this layer was extended the full 24 m width of the backfill mesh and was pinned at the right smooth/rigid boundary (which is a line of symmetry). Although it is not common practise to incorporate such a significantly long reinforcement layer at the base of a wall, this was done to ensure that the extended layer did not fail due to pullout and would intersect any potential slip surface. The reinforcement material properties remained the same as previously described (ultimate strength of 39.7 kN/m and secant tensile stiffness of 400 kN/m). The extended length of the bottom reinforcement layer increased the global stability factor of safety (based on limit equilibrium analysis) from 1.5 to 1.6. The results of the initial analysis with all reinforcement layers 4 m long were compared to the results of the analysis with extended the bottom reinforcement layer (all other layers remaining 4 m long).

It was found that extending the bottom reinforcement layer had no significant effect at any time on the plasticity zones, displacements, vertical or horizontal effective stresses at the base and face of the wall, respectively, or the strains in the reinforcement layers within the reinforced soil block. However, past the end of the reinforced soil block, the strains in the bottom layer increased again to a peak and then decreased towards the boundary. This was found to be due to the extended layer acting as a single reinforcement layer against the development of a potential global failure mechanism around the main reinforced soil block.

5.2. Lengthening, stiffening and strengthening of bottom reinforcement layer

The bottom reinforcement layer was extended to the mesh boundary as described above and the geosynthetic reinforcement strength and stiffness were increased. The reinforcement was taken to be a polyester geogrid with an allowable strength of 759 kN/m (Geotechnical Fabrics Report (GFR), 1999 for Paralink 1250S) based on the ultimate and creep limited strength of the geogrid and accounted for additional installation and durability reductions factors (Table 7). The polyester geogrid secant

Table 7
Geosynthetic material properties for stiffer and stronger base layer

Material property	Test methodology	Paralink 1250S
Ultimate strength (kN/m)	ASTM Standard D 4595	1343
Creep strength (kN/m)	ASTM Standard D 5262	829
Allowable strength (kN/m)	GRI GG4	760
Tensile stiffness (kN/m)	ASTM Standard D 4595	12,000[a]

[a]Based on reported force at 5% strain (Geotechnical Fabrics Report (GFR), 1999).

tensile stiffness was taken to be 12,000 kN/m as reported in the Geotechnical Fabrics Report (GFR) (1999), and was assumed to have limited susceptibility to creep deformation (Koerner, 1990). All other reinforcement layers remained the same as previously described (length of 4 m, ultimate strength of 39.7 kN/m, and secant tensile stiffness of 400 kN/m).

The increased reinforcement length and stiffness increased the global stability factor of safety (based on limit equilibrium analysis) from 1.5 to 2.5. The results of this analysis were compared to that of the extended reinforcement layer with a strength and stiffness of 39.7 and 400 kN/m respectively.

The behaviour of the wall with increased stiffness of the bottom reinforcement layer showed no significant difference from the previous analysis at the EOWC, except for lower strains in the bottom reinforcement layer due to its higher stiffness. Therefore, increasing the stiffness of the bottom layer did not significantly decrease the undrained shear deformations at the EOWC.

After Case 1 loading was subsequently applied, the analysis with the stiffer bottom reinforcement layer showed a noticeable decrease in the displacements at the top, face and base of the wall and a slight decrease in the strains of the main reinforcement layers as compared to the previous case. The decrease in deformations at the top and face of the wall and the reinforcement strains were attributed to the decrease in displacement at the base of the wall. The decreased deformation at the base was due to the higher stiffness of the bottom reinforcement layer increasing the overall stiffness of the backfill at the base and thus decreasing the local deformations at the base of the reinforced section (Fig. 15). Although increasing the stiffness of the reinforcement at the base of the wall did not significantly change the deformation at the base of the wall by 95% consolidation, it did slightly decrease the facing

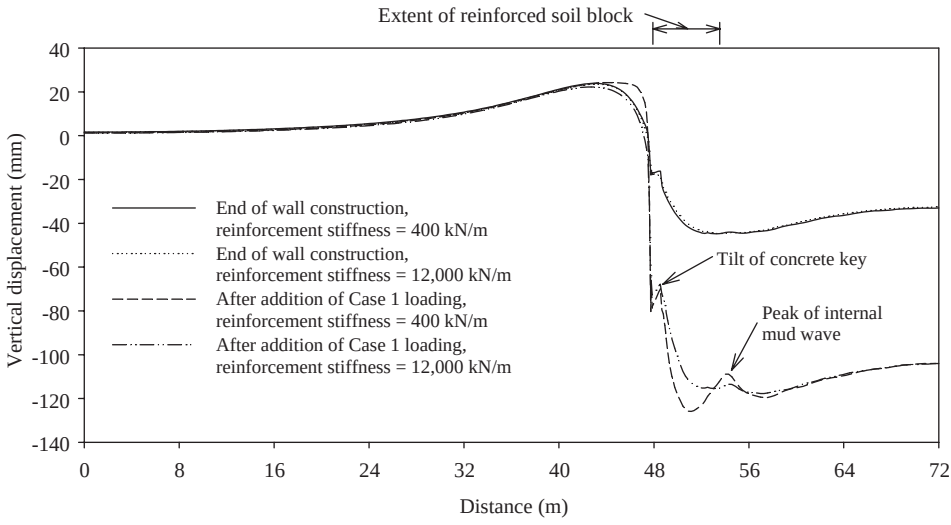

Fig. 15. Vertical displacement at base of wall for extended bottom reinforcement layer with stiffnesses of 400 and 12,000 kN/m.

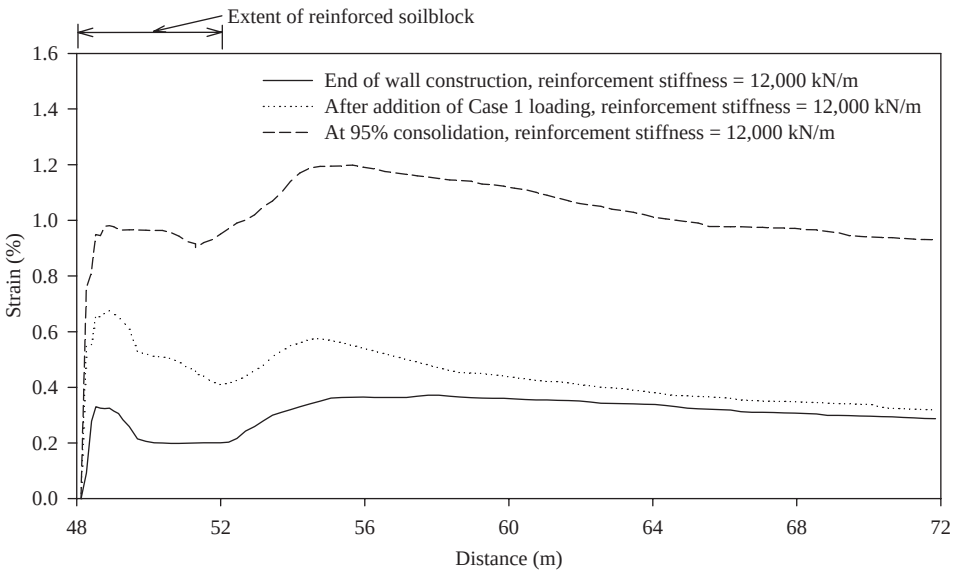

Fig. 16. Strain in extended bottom reinforcement layer with stiffness of 12,000 kN/m (95% consolidation = % degree of consolidation at a point along right lateral boundary at centre of foundation deposit).

displacements and thus the strains in the reinforcement layers. The increased stiffness at the base of the wall also caused the vertical stress at the toe of the wall to slightly increase, as it has been shown to do with a stiffer foundation (Rowe and Skinner, 2001). At the EOWC, the maximum strains (Fig. 16) in the bottom reinforcement layer were higher outside the reinforced soil block than inside the block, thus indicating the critical global failure surface passed behind the main reinforced soil mass. When Case 1 loading was applied, the maximum reinforcement strain was located within the reinforced mass, reflecting the increased load from the abutment and potential bearing failure of the wall. By 95% consolidation the maximum reinforcement strain was again located outside the reinforced soil block, indicating a critical global failure surface around the main reinforced soil mass.

6. Summary and conclusions

The addition of bridge abutment and approach road loading cases at the top of a reinforced wall caused normally consolidated (N/C) yielding and failure, and the development of potential failure mechanisms in the foundation deposit below and around the reinforced soil block. However, the wall and foundation deposit remained stable under both Cases 1 and 2 loadings due to the overall strength of the foundation reflected in external factors of safety greater than unity. The loading scenarios also resulted in a significant increase in the total and differential displacements due to the corresponding N/C consolidation and yielding foundation

behaviour. Although the external stability of the wall did not satisfy the minimum factors of safety, this shows that a geosynthetic reinforced soil wall can withstand the excessive deformations causes by unexpected significant yielding of the foundation soil and even reduce the differential settlement and potential bridge bump effect at the top of the wall.

The increased deformations with load and time correspondingly increased the reinforcement strains. Comparison of the finite-element (FE) predicted and design (National Concrete Masonry Association (NCMA), 1996) calculated strain values in the lower half of the wall showed that the FE analysis predicted strains 60–90% higher for Case 1 loading and 93% and 100% higher for Case 2 loading at 95% consolidation. It was predicted that the forces in the reinforcement layers below the height of 3.6 m increased beyond the allowable reinforcement strength by 95% consolidation for Case 2, and this is not accounted for in conventional design. Although it has been shown that current design methods can be conservative with respect to the expected reinforcement strain (Bell et al., 1983; Bergado et al., 1991, 1994; Nakajima et al., 1996; Allen and Bathurst, 2002), this may not be the case for a wall which experiences significant unexpected yielding of the foundation soil. The internal stability design (National Concrete Masonry Association (NCMA), 1996) for reinforcement rupture only accounts for the applied loading conditions and does not account for the consolidation or shear deformations of the yielding foundation which have been shown to significantly increase reinforcement strains.

The predicted vertical stress at the base of the wall was lower than the value calculated from design, except at the toe of the wall. The vertical stress at the toe was found to be 29% higher on average than the design (National Concrete Masonry Association (NCMA), 1996) values for the wall alone and both Cases 1 and 2 loadings, respectively, likely due to forces transferred from friction along the face and through the reinforcement connections. The stability at the toe of the wall itself should be considered in design as discussed by Skinner and Rowe (2003).

For the cases examined, increasing the length and stiffness of the bottom reinforcement layer in order to increase the bearing capacity and global stability has little overall effect on the behaviour of an already stable wall. The wall had factors of safety of 1.6 and 2.5 against global stability failure for the case of lengthening and the case of lengthening and stiffening the bottom layer, respectively, based on conventional limit equilibrium analysis and the corrected (Bjerrum, 1973) field shear vane strength. Stiffening the bottom reinforcement layer reduced the local and overall undrained shear deformation at the base of the wall under increased loading conditions (Case 1 loading), however, settlements were still large. Extending the reinforcement had an additional stabilizing effect on the backfill soil beyond the reinforced soil block and acted as a reinforcement layer within this section.

Acknowledgements

The research reported herein was funded by the Natural Sciences and Engineering Research Council of Canada (NSERC) and the Ministry of Training, Colleges and

Universities Ontario in the form of an Ontario Graduate Scholarship. The constructive comments of the reviewers were much appreciated.

References

American Association of State Highways and Transportation Officials (AASHTO), 1996. Standard Specifications for Highway Bridges, with 1998 Interims, sixteenth Ed. American Association of State Highway and Transportation Officials, Washington, DC, USA.

Abu-Hejleh, N., Zornberg, J.G., Wang, T., Watcharamonthein, J., 2002. Monitored displacement of unique geosynthetic-reinforced soil bridge abutments. Geosynthetics International 9 (1), 71–95.

Adams, M.T., 2000. Reinforced soil technology at FHWA, making old technology new. Geotechnical Fabrics Report, August, pp. 34–37.

Allen, T.M., Bathurst, R.J., 2002. Observed long-term performance of geosynthetic walls and implications for design. Geosynthetics International 9 (5–6), 525–566.

ASTM Standard D 4595, 1998. Standard test method for tensile properties of geotextiles by wide-width strip method, ASTM, West Conshohocken, PA, USA.

ASTM Standard D 5262, 1998. Standard test method for evaluating the unconfined tensile creep behaviour of geosynthetics, ASTM, West Conshohocken, PA, USA.

Atkinson, J.H., Bransby, P.L., 1978. The Mechanics of Soils, an Introduction to Critical State Soil Mechanics. McGraw-Hill Book Company, England, UK 375 pp.

Bathurst, Jarrett and Associates Inc., 1996. Report on results of Pisa II block unit interface shear capacity testing. Bathurst, Jarrett and Associates Inc., Kingston, Ont., Canada, 5pp.

Bathurst, R.J., 2000. Unpublished test data for ASTM Standard D 4595 stress–strain data for Stratagrid 200. Obtained from Dr. R. Bathurst, Royal Military College, Kingston, Ont., Canada.

Bathurst, R.J., Jones, C.J.F.P., 2001. Earth retaining structures and reinforced slopes. In: Rowe, R.K. (Ed.), Geotechnical and Geoenvironmental Engineering Handbook. Kluwer Academic Publishers, Norwell, MA, USA 1088pp. Chapter 17.

Bell, J.R., Barrett, R.K., Ruckman, A.C., 1983. Geotextile earth-reinforced retaining wall tests: Glenwood Canyon, Colorado. Transportation Research Record 916, 59–69.

Bergado, D.T., Shivashankar, R., Sampaco, C.L., Alfaro, M.C., Anderson, L.R., 1991. Behaviour of a welded wire wall with poor quality, cohesive-friction backfill on soft Bangkok clay: a case study. Canadian Geotechnical Journal 28, 860–880.

Bergado, M.T., Menil N.J.L., Rimoldi, R., Douglas, R.S., 1994. Performance of full scale embankment on soft Bangkok clay with geogrid reinforcement. Proceedings of the Fifth International Conference on Geotextiles, Geomembranes and Related Products, Singapore, pp. 1–4.

Biot, M.A., 1941. General theory of three-dimensional consolidation. Journal of Applied Physics (12), 155–164.

Bjerrum, L., 1973. Problems of soil mechanics and construction on soft and structurally unstable soils (collapsible, expansive and others). Proceedings of the eigth International Conference on Soil Mechanics and Foundation Engineering, Moscow, vol. 3, pp. 111–159.

Bloomfield, R.A., Soliman, A.F., Abraham, A., 2001. Performance of mechanically stabilized earth walls over compressible soils. In: Ochiai, et al. (Eds.), Landmarks in Earth Reinforcement. A.A. Balkema, pp. 317–322.

Bolton, M.D., 1986. The strength and dilatancy of sands. Geotechnique 36 (1), 65–78.

Canadian Foundation Engineering Manual (CFEM), 1992. Canadian Foundation Engineering Manual. third ed. Canadian Geotechnical Society, Richmond, BC, Canada, 512 pp.

Carter, J.P., Balaam, N.P., 1990. Program AFENA, A general finite element algorithm. Centre for Geotechnical Research, University of Sydney, NSW, Australia.

Chen, W.F., Mizuno, E., 1990. Non-linear Analysis in Soil Mechanics—Theory and Implementation. Developments in Geotechnical Engineering, vol. 53. Elsevier Science Publish Company Inc., New York, NY, USA 661pp.

Craig, R.F., 1992. Soil Mechanics, 5th ed. Chapman & Hall, New York, NY, USA 427pp.

Curtis, R.L., Chouery-Curtis, V.E., Miller, D.A., 1988. Geogrid reinforced soil wall on compressible soils. Proceedings of the Second International Conference on Case Histories in Geotechnical Engineering, St. Louis, pp. 1063–1067.

Davis, E.H., Booker, J.R., 1973. The effect of increasing strength with depth on the bearing capacity of clays. Geotechnique 23 (4), 551–563.

Duncan, J.M., Byrne, P., Wong, K.S., Mabry, P., 1980. Strength, stress–strain and bulk modulus parameters for finite element analysis of stresses and movement in soil masses. College of Engineering, University of California, Berkeley.

Esta, J.B., 2001. Reinforced earth ramps over flexible inclusions in Beirut. In: Ochiai, et al. (Eds.), Landmarks in Earth Reinforcement. A.A. Balkema, Rotterdam, pp. 335–340.

Federal Highway Administration (FHWA), 1996. Mechanically stabilized earth walls and reinforced soil slopes, design and construction guidelines. FHWA Demonstration Project 82, Publication Number FHWA-SA-96-071.

Geotechnical Fabrics Report (GFR), 1999. 2000 Specifier's Guide, GFR 17(9), Industrial Fabrics Association International, Roseville, MN, USA.

GRI Standard and Practice, 1991. GG-4 (a&b): Determination of long-term design strength of (stiff and flexible) geogrids. Geosynthetic Research Institute, Drexel University, Philadelphia, PA, USA.

Helwany, S.M.B., Wu, J.T.H., Froessl, B., 2003. GRS bridge abutments—an effective means to alleviate bridge approach settlement. Geotextiles and Geomembranes 21, 177–196.

Holtz, R.D., Kovacs, W.D., 1981. An Introduction to Geotechnical Engineering. Prentice-Hall Inc., Englewood Cliffs, NJ, USA.

Janbu, N., 1963. Soil Compressibility as determined by oedometer and triaxial tests. Proceedings of the European Conference of Soil Mechanics and Foundation Engineering, Wiesbaden, pp. 19–25.

Koerner, R.K., 1990. Designing with Geosynthetics, Fourth Ed. Prentice Hall, Englewood Cliffs, NJ, USA.

Krieger, J., Thamm, B.R., 1991. Studies of failure mechanisms and design methods for geotextile-reinforced soil walls. Geotextiles and Geomembranes 10, 53–63.

Kulhawy, F.H., Mayne, P.W., 1990. Manual on estimating soil properties for foundation design. Research Project 1493-6, Cornell University, Ithaca, New York.

Li, A.L., 2000. Time dependent behaviour of reinforced embankments on soft foundations. PhD Thesis, Faculty of Civil and Environmental Engineering, University of Western Ontario, London, Ontario, Canada, 398pp.

Li, A.L., Rowe, R.K., 1999. Reinforced embankments over soft foundations under undrained and partially drained conditions. Geotextiles and Geomembranes 17 (3), 129–146.

Mesri, G., Lo, D.O.K., Feng, T.W., 1994. Settlement of embankments on soft clays. Keynote Lecture, Settlement '94, Texas A&M University, College Station, TX. Geotechnical Special Publication 40, vol. 1, pp. 8–56.

Nakajima, T., Toriumi, N., Shintani, H., Miyataka, H., Dobahi, K., 1996. Field performance of a geotextile reinforced soil wall with concrete facing blocks. In: Ochiai, H., Yasufuku, N., Omine, K. (Eds.), Earth Reinforcement. Balkema, Rotterdam, Brookfield, pp. 427–432.

National Concrete Masonry Association (NCMA), 1996. Design Manual for Segmental Retaining Walls. Second Ed. NCMA, Herndon, VA, USA.

Perzyna, P., 1963. The constitutive equations for work-hardening and rate sensitive plastic materials. Proceedings of Vibration Problems, Warsaw, vol. 4 (3), pp. 281–290.

Rowe, R.K., Hinchberger, S.D., 1998. The significance of rate effects in modelling the Sackville test embankment. Canadian Geotechnical Journal 35 (3), 500–516.

Rowe, R.K., Skinner, G.D., 2001. Numerical analysis of geosynthetic reinforced retaining wall constructed on a layered soil foundation. Geotextiles and Geomembranes 19, 387–412.

Rowe, R.K., Soderman, K.L., 1987. Stabilization of very soft soils using high strength geosynthetics: the role of finite element analysis. Geotextiles and Geomembranes 6 (1–3), 53–80.

Skinner, G.D., 2002. Geosynthetic reinforced soil walls constructed on yielding foundations. Ph.D. Thesis, Faculty of Applied Science, Queen's University, Kingston, Ont., Canada, 356pp.

Skinner, G.D., Rowe, R.K., 2003. Design and behaviour of geosynthetic reinforced soil walls constructed on yielding foundations. Geosynthetics International 10 (6), 200–214.

Slope/W, 2001. Slope/W for slope stability analysis, from Geo-slope International Ltd., Calgary, Ala., Canada.

Tavenas, F., Jean, P., Leblond, P., Leroueil, S., 1983. The permeability of natural soft clays, Part II: Permeability characteristics. Canadian Geotechnical Journal 20 (4), 645–660.

Terzaghi, K., Peck, R.B., Mesri, G., 1996. Soil Mechanics in Engineering Practice, third ed. Wiley, New York, USA 549pp.

Troung, K.M., Berkebile, M.J., Gladstone, R.A., 2001. Ultra-high hybrid wire and concrete-faced mechanically stabilized earth bridge abutments. In: Ochiai, E., et al. (Eds.), Landmarks in Earth Reinforcement. A.A. Balkema, Rotterdam, pp. 477–481.

Uchimura, T., Tatsuoka, F., Shinoda, M., Tateyama, M., 2001. Preloaded-prestressed geogrid-reinforced soil bridge pier. IGS News 17 (1), 11–13.

Unilock® Armstrong Avenue, Georgetown, Ontario, L7G 4 × 6, Canada.